DOI: 10.1002/chem.200800377

A DFT Study of the Mechanism of Polymerization of ε-Caprolactone Initiated by Organolanthanide Borohydride Complexes

Noémi Barros,[a] Philip Mountford,*[c] Sophie M. Guillaume,*[b] and Laurent Maron*[a]

Abstract: The mechanisms of polymerization of ε-caprolactone (CL) initiated by either the rare-earth hydride [$Cp_2Eu(H)$] or the borohydrides [$Cp_2Eu(BH_4)$] or [$(N_2NN')Eu(BH_4)$] were studied at the DFT level ($Cp = \eta^5$-C_5H_5; $N_2NN' = (2$-$C_5H_4N)CH_2(CH_2CH_2NMe)_2$). For all compounds the reaction proceeds in two steps: a hydride transfer from the rare earth initiator to the carbonyl carbon of the lactone, followed by ring-opening of the monomer. In the last step a difference is observed between the hydride and borohydride complexes, because for the latter the ring-opening is induced by an additional B−H bond cleavage leading to a terminal $-CH_2OBH_2$ group. This corresponds to the reduction by BH_3 of the carbonyl group of CL. Upon reaction of [$Cp_2Eu(H)$] with CL, the alkoxy–aldehyde complex produced, [$Cp_2Eu\{O(CH_2)_5C(O)H\}$], is the first-formed initiating species. In contrast, for the reaction of CL with the borohydride complexes [$(L_x)Eu(BH_4)$] ($L_x = Cp_2$ or N_2NN'), an aliphatic alkoxide with a terminal $-CH_2OBH_2$ group, [$(L_x)Eu\{O(CH_2)_6OBH_2\}$] is formed and subsequently propagates the polymerization. The present DFT investigations are fully compatible with previously reported mechanistic studies of experimental systems.

Keywords: borohydrides • caprolactone • density functional calculations • rare-earth elements • ring-opening polymerization

Introduction

To compensate for the depletion of fossil feed stocks, and to help address global environmental concerns, increasing attention is being paid to polymeric materials synthesized from monomers derived from biomass. In these contexts, the emergence of a wide variety of aliphatic synthetic polyesters prepared through the ring-opening polymerization (ROP) of heterocyclic monomers obtained from renewable resources such as lactone, lactide, or glycolide, is particularly important.[1] Indeed, the development and understanding of controlled "living" polymerization processes leading to biodegradable polymers has become an urgent necessity. Synthetic polyesters are versatile polymers exhibiting good mechanical properties, hydrolyzability, biocompatibility, and eventually biodegradability, which makes them leading candidates for, in particular, biomedical applications (e.g., tissue repair and regeneration, controlled and sustained drug- or gene-delivery vehicles) and recyclable plastics substitutes (e.g., packaging).[1,2]

Of the various ROP processes, such as anionic, cationic, organocatalytic and coordination-insertion, the latter has gained increasing attention, especially when Group 3 initiators, which are less toxic than those involving, for instance, tin or aluminum derivatives, are involved.[1c–g,2,3,4] Considerable efforts are being made to prepare highly sophisticated initiating systems capable of achieving high activity, productivity and stereoselectivity with limited side reactions, in a controlled and "living" process. Within the framework of both traditional metallocene as well as the new generations of "post-metallocene" environments, several types of rare

---

[a] Dr. N. Barros, Dr. L. Maron
Université de Toulouse, INSA,UPS, LPCNO
135 avenue de Rangueil, 31077 Toulouse (France)
Fax: (+33) 561-559-697
E-mail: laurent.maron@irsamc.ups-tlse.fr

[b] Dr. S. M. Guillaume
Laboratoire Catalyse et Organométalliques
CNRS, Université de Rennes 1
Sciences Chimiques de Rennes (UMR 6226)
Campus de Beaulieu, 35042 Rennes Cedex (France)
Fax: (+33) 2-2323-6939
E-mail: sophie.guillaume@univ-rennes1.fr

[c] Prof. Dr. P. Mountford
Chemistry Research Laboratory, Department of Chemistry
University of Oxford, Mansfield Road, Oxford OX1 3TA (UK)
Fax: (+44) 1865-285141
E-mail: philip.mountford@chem.ox.ac.uk

Supporting information for this article is available on the WWW under http://www.chemeurj.org/ or from the author: Complete ref. [19] citation; Cartesian coordinates for the optimized complexes **1**–**21**.

earth complexes have been evaluated. Until recently (see below) these have involved mostly hydride-, alkyl-, alkoxide- or amide-initiating groups or "active bonds".[3,4]

Of special relevance to our present contribution is Yasuda and co-workers' seminal report of the living ROP of ε-caprolactone (CL) by using the bis(pentamethylcyclopentadienyl) lanthanide hydride complex [{Cp*$_2$Sm(μ-H)}$_2$], along with studies of corresponding alkyl and alkoxide lanthanide systems (Cp* = η^5-C_5Me_5).[5] This highly sensitive hydride initiator showed a significantly lower ROP efficiency than the corresponding alkyl complex [Cp*$_2$Sm(Me)(THF)], apparently due to partial deactivation by residual water impurity present in the monomer.[5a] Although [{Cp*$_2$Sm(μ-H)}$_2$] catalyzed the living ROP of CL, the stoichiometric reaction of 0.5 equivalents of [Cp*$_2$Sm(μ-H)]$_2$ with 1 equivalent of CL followed by hydrolysis gave 1,6-hexanediol (1,6-HO-(CH_2)$_6$OH) in 42 % yield based on CL (Scheme 1). Along with the possible formation of [Cp*$_2$SmO(CH_2)$_6$OSmCp*$_2$] as an intermediate in the ROP of CL, as suggested by Yasuda et al., these experimental results might imply that the poly(CL)s formed were α,ω-dihydroxyfunctionalized, but this was not verified experimentally. The formation of HO(CH_2)$_6$OH (Scheme 1) suggests that the initiation step in the ROP of CL by [{Cp*$_2$Sm(μ-H)}$_2$] involves nucleophilic attack of the hydride on the carbonyl carbon atom of the ester through an O−acyl bond cleavage reaction (coordination-insertion). However, the fast rate of this reaction and complications arising from further reaction with [{Cp*$_2$Sm(μ-H)}$_2$] have limited any attempts to probe the mechanism of the process experimentally. No computational studies of the important first step in this ROP process have been described.

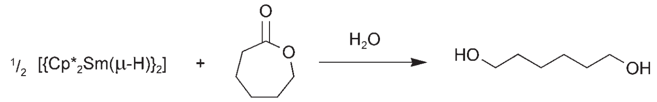

Scheme 1. Stoichiometric reaction of [{Cp*$_2$Sm(μ-H)}$_2$] with CL forming 1,6-hexane diol.[5a]

Although the lanthanide *hydrides* themselves are highly sensitive and prone to dimerization, the corresponding *borohydride* derivatives [(L_x)Ln(BH_4)] (L_x = supporting ligand set) are less so, but still retain considerable hydridic character through one, two or three Ln(μ-H)B linkages.[6] Indeed, borohydride complexes are attracting increasing attention in both organometallic and polymer chemistry (see below) because the BH_4^- ligand exhibits many advantages over other anionic ligands. For example, because it has a comparatively low propensity to form bridging complexes [(L_x)Ln(μ-BH_4)Ln(L_x)], the BH_4^- ligand allows the convenient preparation of well-defined non-aggregated species (unlike the corresponding halide and alkoxide ligands that readily bridge and, as a result, form less-soluble complexes). Although BH_4^- is isosteric with Cl^-, it is much more electron-donating,[7] thus allowing isolation of otherwise unsaturated and inaccessible species. Finally, the BH_4^- ligand is conveniently identified and monitored by ^{1}H and/or ^{11}B NMR spectroscopy. This provides an invaluable "handle" both for the characterization of reaction products as well as for in situ monitoring of experiments in order to identify intermediates and elucidate reaction mechanisms. Although the ground-state bonding and other properties of transition-metal–borohydride compounds have been widely studied by computational methods,[7,8] there are no studies of lanthanide analogues, and none concerning their reactivity in general and in particular in comparison with their [(L_x)Ln(H)] hydride analogues.

In light of this versatility, and following on from the pioneering work of Guillaume,[9–14] a number of well-defined rare earth borohydride complexes[9] have been developed as initiators for the polymerization of polar monomers and especially of cyclic esters.[10–16] Besides being highly efficient and enabling the controlled and "living" ROP of cyclic esters, the most distinctive feature of rare earth borohydrides, and thus their major technological impact, is that they provide easy access to terminally functionalized polymers. This in situ reduction process (see below) provides a direct procedure to prepare α,ω-functionalized polymers, thus avoiding the post-polymerization chemical modification of polymers and all of the associated inherent constraints.

The new α,ω-dihydroxytelechelic PCLs (HO-PCL-OH) were first synthesized using the tris(borohydride) [Ln(BH_4)$_3$(THF)$_3$] (Ln = La, Sm, Nd) and the single-site mono(borohydride) [Cp*$_2$Sm(BH_4)(THF)] complexes as initiators for the ROP of ε-caprolactone.[10a–d] Direct evidence for the presence of a unique type of hydroxyl end group on the polyester was gained from determination of the polymer structure by ^{1}H and ^{13}C NMR spectroscopy and MALDI-TOF analysis. Indirect corroboration of the formation of dihydroxyfunctionalized PCLs was gained from their chemical modification to give the corresponding α,ω-dibromo- (Br-PCL-Br) and α,ω-diamine- (H_2N-PCL-NH_2) functionalized polymers, these being subsequently used as macroinitiators for the successful preparation of AB_2 triblock copolymers, poly(caprolactone)-*b*-[poly(benzylglutamate)]$_2$, and poly(-caprolactone)-*b*-[poly(methyl methacrylate)]$_2$.[12a,13] Finally, diamino-bis(amide)- and -bis(phenoxide)-supported "post metallocene" early lanthanide borohydride compounds were also shown to give α,ω-dihydroxytelechelic PCLs from CL,[15] thus supporting the general nature of the polymerization process and suggesting a common mechanism for all borohydride initiating complexes.

The polymerization mechanism of CL initiated by borohydride complexes has been thoroughly investigated by NMR and IR spectroscopy, in particular by monitoring the stoichiometric reaction of [La(BH_4)$_3$(THF)$_3$] and [Cp*$_2$Sm(BH_4)(THF)] with CL.[10a–d] These analyses allowed identification of several key intermediates (discussed below, see also Scheme 2) that were isolated and characterized. Additional evidence for the presence of −CH_2OBH_2 groups (that lead to the formation of a "physical gel") during the polymerization process was obtained from IR investigations that

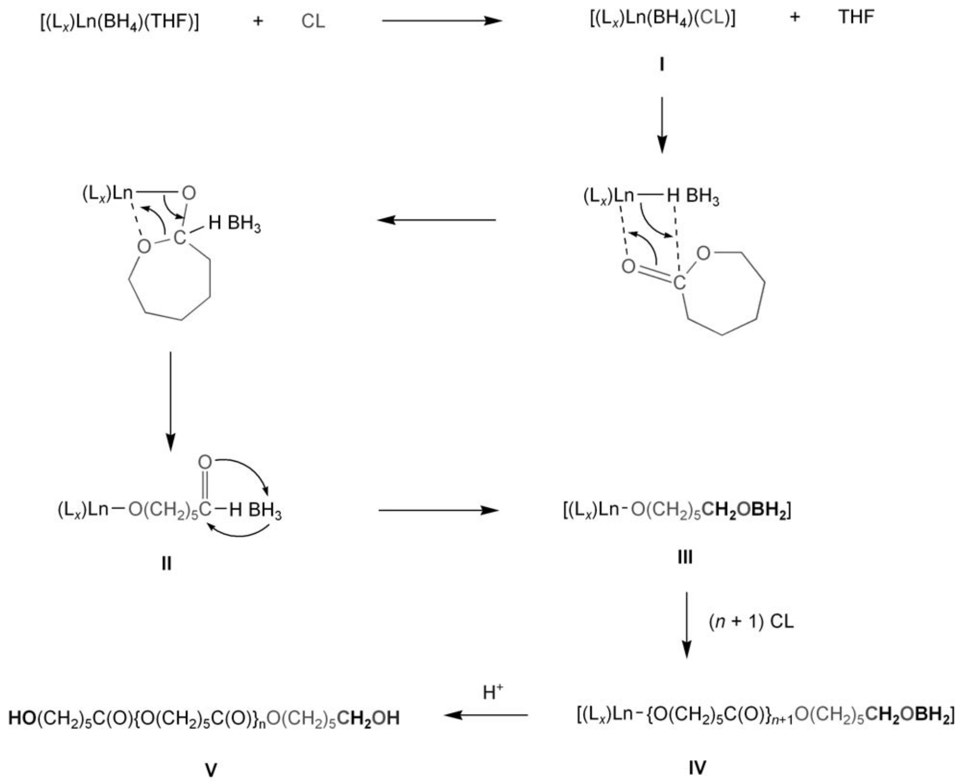

Scheme 2. Proposed general mechanism for the polymerization of ε-caprolactone initiated by $[(L_x)Ln(BH_4)(THF)]$.[10a–d]

unambiguously showed the presence of B−H unit(s) in the relevant intermediates depicted in Scheme 2.[10c]

From these observations, a mechanism common to borohydride initiators $[(L_x)Ln(BH_4)(THF)]$ ($L_x = Cp^*_2$, $(2\text{-}C_5H_4N)CH_2(CH_2CH_2NSiMe_3)_2$), or a related diamido-bis(phenoxide) ligand,[15a] was suggested to rationalize the formation of the second hydroxyl end-function (Scheme 2).[10a–d] This involved initial displacement of the coordinated THF from the metal by CL to form the adduct $[(L_x)Ln(BH_4)(CL)]$ (**I**). Subsequently, this first monomer molecule inserts into the Ln−BH$_4$ bond with a C(O)−O (oxygen–acyl) bond cleavage to give the intermediate $[(L_x)Ln\{O(CH_2)_5C(O)H{\cdot}BH_3\}_3]$ (**II**, most likely solvated by a Lewis base). The displaced BH_3 group immediately reduces the adjacent aldehyde function to form a $-CH_2OBH_2$ group, thus generating an alkoxyborane derivative $[(L_x)Ln\{O(CH_2)_5CH_2OBH_2\}]$ (**III**). Subsequent coordination-insertion polymerization through the Ln−O bond of this species gives the active polymer $[(L_x)Ln\{\{O(CH_2)_5C(O)\}_{n+1}O(CH_2)_5CH_2OBH_2\}]$ (**IV**). Finally, upon quenching and deactivation, hydrolysis of the Ln−O and $CH_2O{-}BH_2$ bonds of **IV** generates an hydroxyl end group at each chain end giving $HO(CH_2)_5C(O)\{O(CH_2)_5C(O)\}_nO(CH_2)_6OH$, HO-PCL-OH (**V**). As mentioned above, direct experimental evidence has been obtained for species of types **I**, **III**, **IV** and **V** in both mono- and tris(borohydride) systems.[10a–d]

Theoretical investigations of chemical reactivity have been successfully applied in 4f-elements chemistry[8a,14,17,18] and recently on radical polymerization of acrylates.[18c–d] However, despite the emerging importance of Group 3 or lanthanide ROP catalysts, theoretical studies of such systems are particularly scarce.[14,18b]

We very recently used DFT to gain important insights into the commercially important synthesis of poly(methylmethacrylate) (PMMA) initiated by rare earth borohydride and hydride complexes.[14] This study of the polymerization of MMA initiated by metallocene and non-metallocene lanthanide borohydride systems (modeled as $[Eu(BH_4)_3]$ and $[Cp_2Eu(BH_4)]$ ($Cp = \eta^5\text{-}C_5H_5$)) established the underlying influences of the ligands on the energetics and competing pathways of the reaction. The study was further extended to the model hydride complex $[Cp_2Eu(H)]$, for which experimental results were also available for the corresponding real system $[\{Cp^*_2Sm(\mu\text{-}H)\}_2]$, and accounted for the very different abilities of the borohydride and hydride initiators in the production of poly(MMA).

In this paper, we present comparative DFT investigations of the ROP of ε-caprolactone initiated by the hydride complex $[Cp_2Eu(H)]$ and the borohydride systems $[Cp_2Eu(BH_4)]$ and $[(N_2NN')Eu(BH_4)]$ ($N_2NN' = (2\text{-}C_5H_4N)CH_2(CH_2CH_2NMe)_2$). Although they are consistent with previous experimental observations of the real systems (see above), these computational results also allow a deeper insight into the thermodynamic and mechanistic features of the initial steps in the ROP of CL using contrasting hydride-type initiators in different ligand environments. Comparisons are thus made between hydride and borohydride active Ln−X (X = H, BH_4) bonds, and between metallocene and "post-metallocene" supporting ligand–metal fragments.

Computational Details

All the calculations were performed with the Gaussian 03[19] suite of programs. For technical reasons associated with the difficulty of employing effective core potentials (ECPs) with an odd number of core electrons with Gaussian 03, the samarium atoms, used experimentally, were replaced by europium atoms. It should be noted that there were no problems with Gaussian 98. According to previous theoretical studies, the change from Sm to Eu leads to minimal modifications in the calculated geometric and energetic data.[18] Europium was treated with a Stuttgart–Dresden pseudopotential that includes the 4f electrons in core, in combination with their adapted basis set.[20] In all cases, the basis set was augmented by a set of f-polarization functions.[21] Carbon, oxygen, and hydrogen atoms are described with a 6–31G(d,p) double-ζ basis set.[22] Calculations were carried out at the density functional theory (DFT) level of theory using the hybrid functional B3PW91.[23] Geometry optimizations were carried out without any symmetry restrictions and the nature of the extrema (minima and transition states) was verified by analytical frequency calculations. The calculations were carried out in the gas phase. The free energies were computed at $T = 298.15$ K within the harmonic approximation.

Results and Discussion

Polymerization of CL initiated by [Cp*$_2$Sm(H)]: Computational study of two possible reaction mechanisms

In this study the Sm centers were replaced by Eu for technical reasons associated with the use of f-in-core effective core potentials with an even number of core electrons (see Computational Details). In the following, and based on previous studies,[14,17] the Cp* ligand was replaced by Cp. Even though it is known that [Cp*$_2$Sm(H)] is a dimer in the absence of coordinating species, it has been shown both experimentally[5] and theoretically[17c–d] that the monomer is the active species.

Two pathways (denoted "(a)" and "(b)" in Scheme 3) were envisaged previously for the opening of the lactone ring from an *alkoxide*-propagating center (L$_x$)Ln-OR.[1c,e,24] Thus, ring-opening can proceed through an oxygen–alkyl (C$_\beta$–O, path (a)) or an oxygen–acyl (C(O)−O, path (b)) bond cleavage, resulting in the formation of carboxylate or alkoxide active centers, respectively, as illustrated in Scheme 3. Larger lactones (six- and seven-membered rings, i.e., δ- and ε-lactones, respectively) such as CL ring-open only by nucleophilic attack of the OR$^-$ anion on the carbonyl carbon with C(O)−O bond cleavage, however, the opening of four-membered rings (β-lactones such as β-propiolactone (PL)) may occur through both a C$_\beta$−O and a C(O)−O bond-scission pathway. The differences in reactivity were rationalized by the impact of the stereochemistry of the ring on the nucleophilic attack, the puckered CL ring does not affect it, whereas the flat PL cycle hinders it.[1a,e,24] Also, based on ab initio MO calculations, the conformation was found to be most energetically favorable with CL rather than with PL.[24b] To gain further insights into these findings, the two ring-cleavage mechanisms were considered in the DFT investigations of the polymerization of CL initiated by Cp$_2$Eu(H).

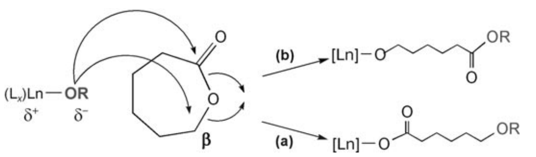

Scheme 3. Possible ring-openings of CL through oxygen–alkyl (a) and oxygen–acyl (b) bond cleavages from an alkoxide initiating center.[1c,e,24]

O−*Acyl (C(O)*−*O) ring-opening of CL: Classical and favored mechanism*: The free-energy profile determined for the reaction of CL with [Cp$_2$Eu(H)], **1**, is presented in Figure 1. The three distinctive features of this ring-opening reaction are: the stepwise process revealed by the calculations; the exergonic character of all the various intermediates involved; the effective ring-opening, which only occurs within the second step. Overall, the reaction is calculated to be exergonic by 38.7 kcal mol^{-1}, which means that the formation of the alkoxy–aldehyde complex [Cp$_2$Eu{O-(CH$_2$)$_5$C(O)H}], **7**, from [Cp$_2$Eu(H)] and CL is thermodynamically favorable. From the kinetic point of view, the two transition states (TS) **3** and **6** are found to be at rather low energy, leading to an overall facile reaction. Thus, this reaction seems, on the whole, to be favorable.

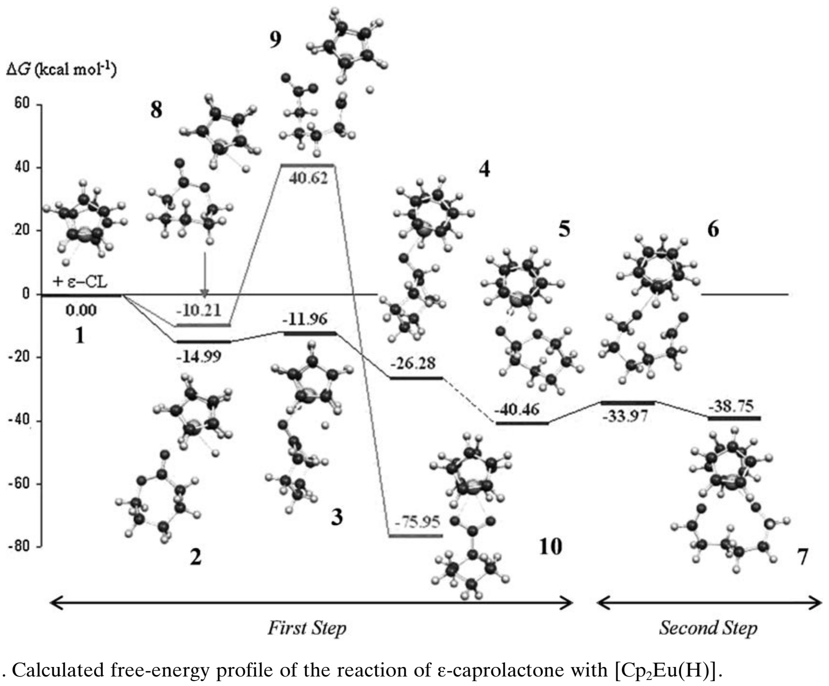

Figure 1. Calculated free-energy profile of the reaction of ε-caprolactone with [Cp$_2$Eu(H)].

The first step of the reaction corresponds to the C=O double insertion into the Eu−H bond of **1** to form **5**. All of the optimized structures for this process (complexes **1**–**5**) are given in Figure 2. The 1,2 insertion of π systems into a Ln−H bond has been extensively studied both theoretically and experimentally, either with olefins or with C-heteroatom bonds, and it is now well established that these reactions are kinetically facile and thermodynamically slightly exergonic.[25,24] As expected, we found this step (**1**→**4**) to be kinetically accessible, with an activation barrier lower than the energy of the separated **1** and CL, and thermodynamically favorable (26.3 kcal mol^{-1} below the separated reactants and 11.3 kcal mol^{-1} below the adduct **2**).

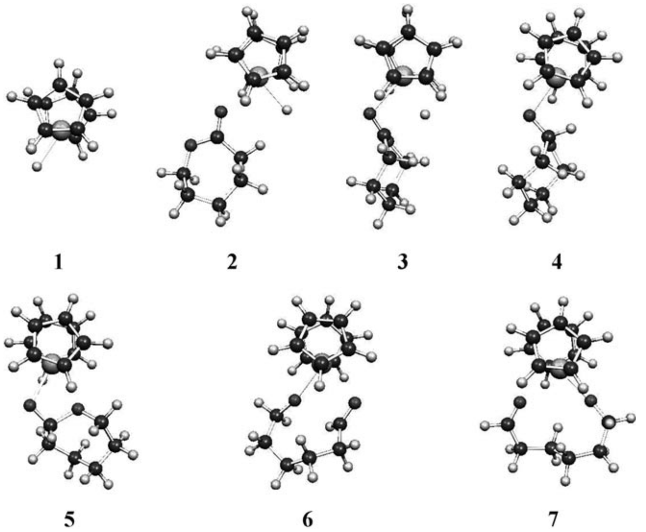

Figure 2. Optimized structure of complexes **1**–**7** involved in the first step of the reaction of CL with [$Cp_2Eu(H)$] (O−acyl ring-opening).

The reaction between [$Cp_2Eu(H)$] and CL starts by formation of the [$Cp_2Eu(H)(CL)$] adduct **2**, in which CL interacts with the metal center through the exocyclic carbonyl oxygen atom. This adduct formation is exergonic by 15.0 kcal mol^{-1}, in agreement with a stabilizing electrostatic interaction between the negatively charged oxygen of the carbonyl and the positive lanthanide center (−0.74 and +2.37, respectively), further supported by the quite short Eu−O distance (2.44 Å). Also, the C−O bond is only marginally elongated with respect to a free CL (+0.03 Å), as is the Eu−H distance (+0.02 Å) with respect to [$Cp_2Eu(H)$]. In adduct **2**, the CL ring adopts a chair conformation without any interaction between the intracyclic oxygen and the metal center. This is in agreement with the previously mentioned ab initio MO findings.[24b]

Adduct **2** leads to a quite early insertion TS, **3**, lying only 3.0 kcal mol^{-1} above **2** (12.0 kcal mol^{-1} below the separated reactants). In agreement with this small energy difference, both **2** and **3** display very similar geometries. Thus, the reaction from [$Cp_2Eu(H)$] and CL to reach TS **3** is kinetically very easy. Indeed, despite the rotation by 90° of the CL around the Eu···O bond and a slight pyramidalization of the carbon atom, none of the other geometrical parameters are significantly affected on going from **2** to **3**. The most modified bond is Eu−H, which is elongated by only 0.09 Å, whereas the Eu···O and C=O lengths are shortened by 0.06 Å and elongated by 0.02 Å, respectively. The (O)C−H bond about to form is still long, 2.19 Å. As indicated above, the CL ring in **3** is now perpendicular to the equatorial plane of the [$Cp_2Eu(H)$] fragment and the chair conformation of the ring is retained. Such a TS for the insertion of a C=O double bond into a Ln–H moiety has already been reported to occur with a low activation barrier.[26]

TS **3** evolves toward a cyclic alkoxide product **4** lying 14.3 kcal mol^{-1} below it. In **4**, the CL ring is still perpendicular to the equatorial plane. The Eu···H distance of now 2.50 Å is in agreement with a broken bond, yet also with a remaining Eu···H interaction, such as an agostic one. This interaction is further confirmed by the length of the formed C−H bond (1.16 Å), which is 0.07 Å longer than a standard C−H bond. The Eu−O bond is now formed (2.18 Å) and the C−O bond has elongated to 1.35 Å indicating a more pronounced single-bond character.

Interestingly, this cyclic alkoxide intermediate **4** is calculated to be fairly stable, mostly due to the strong electrostatic interaction between the alkoxy group and the metal center, with some contribution from the agostic Eu···H interaction. Analysis of this intermediate clearly showed that a rotation of 90° around the O−Eu bond would lead to a less-sterically crowded complex and would allow the favorable coordination of the intracyclic oxygen. Despite our efforts, it was not possible to locate the rotation TS, but rather a new minimum as complex **5**, exhibiting a coordination of the intracyclic oxygen, was obtained. This complex is calculated to be stabilized by 14.2 kcal mol^{-1} with respect to complex **4**. Notably, the Eu−O distance has been slightly increased by 0.04 Å during the rotation process, but the C−O distance remains the same as in complex **4** (1.35 Å). The Eu···O(intracyclic) distance is 2.47 Å, indicating an interaction between a lone pair of electrons on the O and the metal center. Moreover, it should be noticed that this intermediate **5** can undergo ring-opening, as the O(intracyclic) is coordinated to the metal center, which is not the case for intermediate **4**.

Thus, in a second step, starting from intermediate **5**, the two possibilities to open the ring were considered. All the optimized structures for this step (**5**–**7**) are included in Figure 2. From the alkoxide–ether complex **5**, a CH(OEu)−OCH_2 ring-opening bond cleavage can occur. Indeed, complex **5** connects to TS **6**, which is 6.5 kcal mol^{-1} above **5**, in agreement with a kinetically accessible reaction. This TS can be described as an isomerization of a metallated cyclic alkoxide–ether into a linear alkoxide–aldehyde. Thus, at the TS **6**, the CH(OEu)···OCH_2 distance is elongated by 0.93 Å from 1.52 to 2.45 Å, showing clearly that the bond is effectively broken. Thus, the nature of the two oxygen atoms is changing. Indeed, the formerly intracyclic $OC_\beta H_2$ is now in closer interaction with the metal center (Eu−O distance of 2.19 Å in **6** compared to 2.47 Å in **5**), becoming a Eu−OCH_2

alkoxide group, whereas the former alkoxide–oxygen is becoming more Lewis base/aldehyde-like (Eu–O distance of 2.45 Å in **6** compared to 2.22 Å in **5**). This is further confirmed by the shortening of the C–O distance by 0.09 Å leading to a C=O double bond in **6**. However, the aldehyde carbon in **6** is not yet fully planar and still oriented toward the formerly intracyclic $OC_\beta H_2$.

TS **6** connects to the final alkoxide–aldehyde complex $[Cp_2Eu\{O(CH_2)_5C(O)H\}]$, **7**, calculated to be +1.7 kcal mol^{-1} above **5**, thus leading to a slightly endergonic step. In fact, this value is so small that this step can be considered as athermic. Complex **7** closely resembles the previously described TS **6**. Indeed, with respect to **6**, only the $H(O)C\cdots OCH_2$ distance has increased up to 4.13 Å, whereas the Eu–OCH_2 distance has slightly reduced to 2.12 Å, and the terminal aldehyde group, which has rotated to allow interaction between the carbonyl oxygen and the metal center, is now planar.

A natural bonding analysis (NBO) of complex **7** clearly indicates a charge separation with negative charge located on the alkoxide and on the oxygen of the aldehyde groups and the positive charge located on the metal center. Thus, solvent effects, even in the case of less-polar ones such as toluene, would stabilize complex **7** more than complex **5** leading to an overall athermic-to-slightly exergonic reaction. Furthermore, because the energy of this reaction is quite small, one could certainly speculate whether the CH(OEu)–OCH_2 bond-cleavage process might be promoted by the coordination of a second CL molecule to **5**. Thus, the coordination of a second CL molecule to complexes **5** and **7** was computationally investigated. The structures obtained are presented in Figure 3. In both **5(CL)** and **7(CL)** adducts, the CL molecule is coordinated to the metal center by the exocyclic carbonyl oxygen. This coordination appears to be energetically marginally favorable for complex **5** (stabilization of 3.2 kcal mol^{-1}), but not for complex **7** (destabilization of 1.6 kcal mol^{-1}), presumably due to the larger "bite angle" for the bidentate $O(CH_2)_5C(O)H$ ligand. Thus, the coordination of a second CL molecule does not appear to influence the ring-opening process from a thermodynamic perspective.

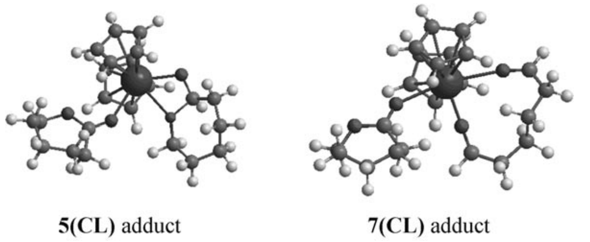

Figure 3. Optimized structure of the ε-caprolactone adduct to the closed and opened complexes **7(CL)** and **5(CL)**, respectively.

Thus, it can be concluded that ring-opening can occur through the mechanism proposed in Figure 1 (pathway **1**→**7**). Because the last ring-opening of **6** into **7** appears almost athermic, suggestive of the absence of a clear thermodynamic preference for the ring-opening mode, the other ring-opening possibility, namely a C_β–O bond-scission pathway (see path (a) in Scheme 3) was considered in order to gain some thermodynamic and kinetic insights into this process.

O–Alkyl (C_β–O) ring-opening of CL: Unlikely mechanism: The calculated free-energy profile for this C_β–O bond-scission mechanism is presented in Figure 1 (pathway **8**→**10**). The reaction between $[Cp_2Eu(H)]$, **1**, and CL involving a C_β–O bond scission is highly exergonic by 76.0 kcal mol^{-1}, but kinetically difficult (activation barrier of 40.6 kcal mol^{-1} with respect to separated **1** and CL). This O–alkyl cleavage of the monomer is predicted to lead ultimately to the formation of the chelating carboxylate $[Cp_2Eu\{O_2C(CH_2)_4Me\}]$, **10**. A similar energy profile leading to the formation of this carboxylate species from the reaction of $Cp_2Eu(H)$ and MMA was also found to be thermodynamically highly favorable with a quite high activation barrier, the latter being rationalized by the S_N2-like reaction involving a planar alkyl group at the TS.[14]

The present reaction involves first the exergonic (by 10.2 kcal mol^{-1}) formation of adduct, **8**. Complex **8** differs from adduct **2** in that the CL interacts with the metal center through both oxygen atoms instead of only one. Interestingly, the coordination of the two oxygen atoms slightly destabilizes **8** (by 4.8 kcal mol^{-1}) relative to **2**. This can be explained by the fact that in **8** the two Eu–O distances are approximately equal (2.68 Å) but longer than the one in **2** (2.44 Å). This leads to a smaller electrostatic interaction between the exocyclic oxygen, which is the most negatively charged, and the metal center. This smaller interaction is not balanced by the additional interaction between the intracyclic oxygen and the metal center. The important negative charge of the exocyclic oxygen is further supported by a NBO analysis (−0.65 e), which is smaller than for **2**, namely −0.74 e. Furthermore, the C=O bond is rather long (1.34 Å).

As for **2**, the CL ring is puckered in **8** and the O–C(O) chelating part of the CL is lying in the equatorial plane of the $\{Cp_2Eu\}$ fragment. However, in **8** the intracyclic oxygen is facing the hydride (Figure 4). This adduct connects to the TS **9**, which leads eventually to C_β–O(intracyclic) bond scission (giving product **10**). The TS **9** lies some 50.8 kcal mol^{-1} above **8** (ca. 40.6 kcal mol^{-1} above the separated reactants). The C_β–O bond scission is thus calculated to be almost ki-

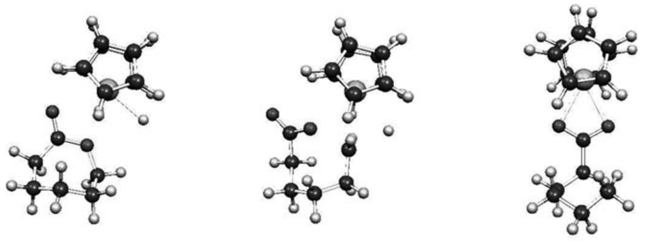

Figure 4. Optimized structures of complexes **8**–**10** involved in the second step of the reaction of CL with $[Cp_2Eu(H)]$ (O–alkyl ring-opening).

netically impossible. TS **9** clearly indicates a S_N2-type TS in which the $-CH_2CO_2^-$ and H^- anions (each bound to Eu) are the leaving group and nucleophile, respectively. In the TS, the C_β carbon has a distorted trigonal-bipyramidal geometry, but with a O···C···H angle of approximately 126° in contrast to the ideal 180°. The Eu–H distance in **9** has elongated to 2.30 Å and the newly formed C_β···H bond is still long (1.96 Å). The C_β···O distance is also long (1.96 Å) and, as expected for a S_N2-type TS, it is equal to the new C···H. At the same time, the Eu–O(intracyclic) distance has decreased only slightly by 0.04 Å with respect to **8**, whereas the favorable exocyclic O···Eu interaction has lengthened substantially from 2.68 to 4.12 Å. The height of the barrier is clearly due to the planarity of the CH_2R group (as found in the MMA polymerization case)[14] and the considerable geometric distortions required to achieve this TS.

Notably, the charges are very well separated in a S_N2 TS so that **9** could be stabilized by a solvent of such low polarity as toluene. Indeed, solvent-stabilization effects in **9** were estimated by a single-point calculation to be 15 $kcal\,mol^{-1}$. However, this stabilization does not make this TS competitive with the one determined in the other pathway (**2**→**4** via TS **3**).

As mentioned, TS **9** evolves to form the carboxylate complex $[Cp_2Eu\{O_2C(CH_2)_4Me\}]$, **10**, which is calculated to be highly exergonic by 116.6 $kcal\,mol^{-1}$ with respect to the TS (and 76.0 $kcal\,mol^{-1}$ with respect to the separated reactants). The carboxylate ligand interacts with the lanthanide center in a highly favorable bidentate fashion with equal Eu–O distance (2.38 Å). An NBO analysis clearly indicates that the negative charge is delocalized between the two oxygen atoms and the complex is stabilized by an electrostatic interaction with the electropositive metal center as expected. The C–H bond is now fully formed (1.10 Å).

Our computational results are in full agreement with the experimental data (see Introduction) reported by Yasuda et al. for the polymerization of CL by $[\{Cp^*_2Sm(\mu\text{-}H)\}_2]$.[5] Our calculations explain why initiation should proceed through the "classical" O–acyl ring-opening (C(O)–O bond cleavage) leading to an alkoxide–aldehyde species $[Cp^*_2Sm\{O(CH_2)_5C(O)H\}]$ analogous to complex **7**. They also give unique insight into why the potentially competitive C_β–O bond-scission process is *not* observed. Finally, we recall that, experimentally,[5] reaction of $[\{Cp^*_2Sm(\mu\text{-}H)\}_2]$ (0.5 equiv) with CL (1 equiv) affords the doubly reduced CL product $[Cp^*_2SmO(CH_2)_6OSmCp^*_2]$. Our calculations further suggest that this reduced complex might arise from attack of $[Cp^*_2Sm(H)]$ on the initially formed alkoxide–aldehyde $[Cp^*_2Sm\{O(CH_2)_5C(O)H\}]$ (modeled by **7**, Figures 1 and 2).

Polymerization of CL by metallocene and non-metallocene borohydride complexes

As detailed in the Introduction, the borohydride complexes offer very different CL polymerization reactivity patterns as a consequence of the reducing potential of the BH_4^- ligand. This has now been established for a range of initiators: the "simple" inorganic tris(borohydrides) $[Ln(BH_4)_3(THF)_3]$, the metallocene $[Cp^*_2Sm(BH_4)(THF)]$ and, subsequently, several post-metallocene systems such as $[(N_2NN^*)Sm(BH_4)(THF)]$ ($N_2NN^* = (2\text{-}C_5H_4N)CH_2(CH_2CH_2NAr)_2$) or bis(phenoxide) analogues.[10a–d,15] It was, therefore, of utmost interest to compare the DFT results of the initiation step of CL polymerization from the hydride $[Cp^*_2Sm(H)]$ (using the model $[Cp_2Eu(H)]$) to those from the corresponding metallocene–borohydride derivative $[Cp^*_2Sm(BH_4)(THF)]$ (using the model $[Cp_2Eu(BH_4)]$). Furthermore, because the beneficial effect of using alternative supporting ligands in catalytic systems is well established,[10b,27] we also undertook a study of a representative post-metallocene system for comparison with the metallocene analogues. This will certainly aid further research in this area. A study of the tris(borohydrides) $[Ln(BH_4)_3(THF)_3]$ was not carried out for reasons of computational efficiency. Furthermore, in our results for the borohydride-initiated polymerization of MMA, no important reactivity differences between the model $[Eu(BH_4)_3(THF)_3]$ and $[Cp_2Eu(BH_4)]$ systems was found computationally.[14] These in silico explorations are further in line with our efforts to understand the ability of borohydride catalysts to efficiently polymerize cyclic esters.[10,11,14]

Polymerization of CL initiated by $[Cp^*_2Sm(BH_4)(THF)]$: Comparison of hydride and borohydride–metallocene systems: The calculations with $[Cp_2Eu(H)]$ revealed that the C(O)–O (O–acyl) cleavage was kinetically and thermodynamically favorable, whereas the C_β–O (O–alkyl) cleavage route was highly kinetically disfavored, leading to catalytically inactive systems. Moreover, the ring-opening was shown experimentally to occur through O–acyl cleavage.[10a–d] Also, in our previous study on MMA polymerization, we showed that formation of the corresponding carboxylate species was also kinetically disfavored.[14] Therefore, only the O–acyl cleavage mechanism was investigated for the borohydride complexes. The calculated pathway along with all the optimized structures are depicted in Figures 5 and 6.

As observed with $[Cp_2Eu(H)]$, **1**, the reaction of $[Cp_2Eu(BH_4)]$ with CL proceeds in a stepwise manner and the CL ring only opens in the second step (**13**→**15**, Figure 5). The calculated activation barriers are rather low (maximum of 15.5 $kcal\,mol^{-1}$ with respect to the separated reactants) and the overall reaction is thermodynamically favorable (formation of **15**, exergonic by 29.0 $kcal\,mol^{-1}$). It should, however, be noticed that these two values are higher than in the hydride case. A similar comparative situation was found for the MMA polymerization, indicating that the borohydride catalysts are initiating more slowly than the hydride homologues. However, because the second step of the reaction with the hydride is almost athermic (**5**→**7**, Figure 1), the use of borohydride catalyst turns the ring-opening into a firmly exergonic step (**13**→**15**, Figure 5) with respect to the cyclic alkoxide intermediate **13**. This might lead to a better control of the polymerization process with borohydride complexes.

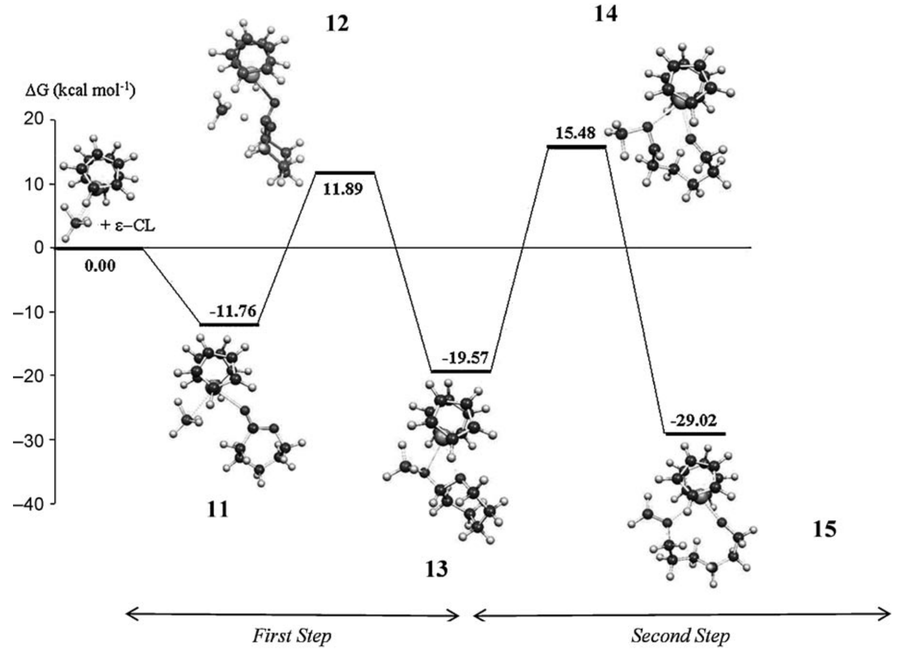

Figure 5. Calculated free-energy profile for the reaction of ε-caprolactone with [$Cp_2Eu(BH_4)$].

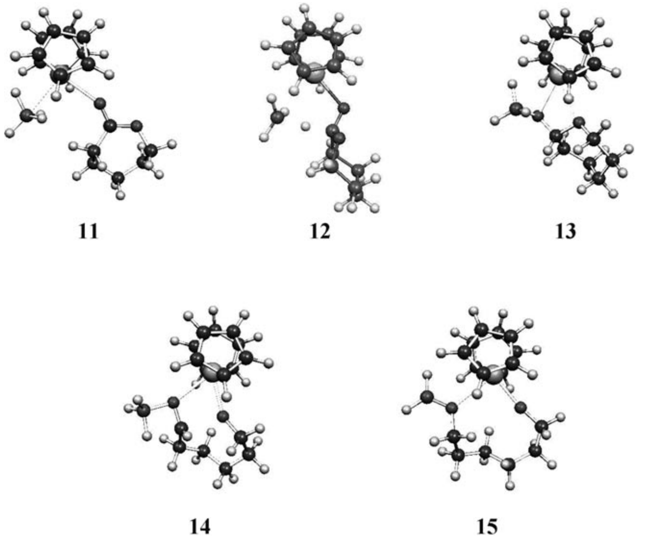

Figure 6. Optimized structures of complexes **11**–**15** involved in the first and second steps of the reaction of CL with [$Cp_2Eu(BH_4)$] (O−acyl ring-opening).

As mentioned above, and as in the hydride case, the first step of the reaction (up to **13**) does not lead to the ring-opening of CL. In the first step, the reaction begins with the formation of the adduct [$Cp_2Eu(BH_4)(CL)$], **11**. As within the hydride adduct **2**, the CL interacts with the metal center through the exocyclic carbonyl oxygen. This adduct is 11.8 kcal mol^{-1} below the entrance channel, indicating a relatively strong Eu···(O)C interaction. The slight difference to the value obtained with **2** (15 kcal mol^{-1}) could be attributed to the tridentate coordination of the borohydride ligand to the metal center. The CL ring in **11** is lying in the equatorial plane of the Cp_2Eu complex with a chair-like conformation, in a very similar way to that observed with the hydride **2**. This adduct **11** connects to a TS, **12**, which lies 23.7 kcal mol^{-1} above it (11.9 kcal mol^{-1} above the separated reactants).[28] Thus, this step appears kinetically favorable. Species **12** corresponds to the TS for the hydride transfer from the coordinated BH_4^- ligand to the C=O group carbon of CL. The BH_3 group, which is pyramidalized, is at a B···H distance of 1.56 Å from the migrating H^-. Although the B···H^- distance is quite long, some electron density remains on the hydrogen atoms of the remaining BH_3 group, in agreement with the observed η^1-coordination of the BH_3 to the metal center (ca. 1.1–1.2 Å).[6a] This is also consistent with the ability of borohydride ligands to interact with metal fragments in either a η^1, η^2, or η^3 fashion.[6,7] At the same time as the H^- is migrating, the CL ring rotates by approximately 90° around the C=O···Eu bond and the C is pyramidalized backward to orient the 2p orbital on C towards the migrating hydride. The C=O has been elongated (1.30 Å), thereby localizing the negative charge on the oxygen (the NBO analysis indicates a charge of −0.90 e on this oxygen), leading to a formal empty 2p orbital at the carbon atom. As in the hydride case, the chair conformation of the ring is maintained and the intracyclic oxygen is not interacting with the metal center (3.73 Å).

The TS **12** connects to an alkoxide–borate complex **13**, calculated to be exergonic by 19.6 kcal mol^{-1} (with respect to the separated reactants) and is very similar to the one obtained previously in the hydride case (**4**, Figures 1 and 2). The major difference is that the formed BH_3 adds to the exocyclic oxygen leading to a borate complex, which is interacting with the metal center through two hydrogen atoms. The ring has rotated around the Eu···O(C−O) bond to allow interaction between the intracyclic oxygen and the metal center. Thus, the conformation of the ring is maintained. This first step of the reaction is quite similar to the one described with the hydride (**1**→**5**), but is less favored from both a thermodynamic and kinetic point of view.

The second (ring-opening) step starting from the borate complex **13** (up to **15**) does not require the rotation of CL as in the hydride case, even though this process is energetically costless. This borate complex **13** connects to TS **14**, which lies 35.1 kcal mol^{-1} above it (15.5 kcal mol^{-1} below separated reactants), leading to an overall facile reaction. The geometry of the TS is quite interesting in that the borate complex does not interact with the metal center through the BH_3 group, but rather through the oxygen. One of the B–H bonds is slightly elongated (1.26 Å) and is oriented toward the C=O carbon atom. The B–H···C angle is close to 90°, clearly indicating an interaction between H and C. Similarly, the C-O-B angle is also around 90° to allow a stronger C···H interaction. At the same time, the C(O)–O(endocyclic) bond is breaking (2.13 Å), finally leading to the opening of the ring. The exocyclic O(acyl) has accumulated a significant negative charge (−0.97 e) and is acting as an alkoxide group. Thus, unlike that which is observed with the hydride case, the ring-opening occurs through a *second* B–H hydride transfer and formation of an additional C–H bond.

Indeed, following the intrinsic reaction coordinates leads to the formation of an aliphatic alkoxide with a terminal $-CH_2OBH_2$ group, namely $[Cp_2Eu\{O(CH_2)_5CH_2OBH_2\}]$, **15**, which lies 44.5 kcal mol^{-1} below TS **14** (29.0 kcal mol^{-1} below the separated reactants). Thus, this second step is thermodynamically favored making the overall reaction thermodynamically possible. This is the main difference from the hydride case in which the second step is athermic, leading to a possible equilibrium between the closed and opened complexes. This can be attributed to the formation of the terminal CH_2OBH_2 group that is driving the reaction energy down. Chemically, this corresponds to BH_3 reduction of the aldehyde group of **7** (Figure 1), *a reaction that cannot occur in the hydride case*, except by reaction with a second equivalent of metal hydride $[Cp^*_2Sm(H)]$, as observed experimentally. Thus, the ring-opening/initiation reaction is more easily thermodynamically controlled by the borohydride complex $[Cp_2Eu(BH_4)]$ because no quasi-equilibrium is involved, although the activation barriers are higher than in the hydride case. The calculated most-favorable complex formed from the reaction of $[Cp_2Eu(BH_4)]$ with CL, the alkoxide–borate **15**, thus exactly matches the postulated active species **III** (Scheme 2).

Polymerization of CL initiated by [(N_2NN^*)Sm(BH_4)(THF)]: Comparison with a non-metallocene system: Following the success of the metallocene complex $[Cp^*_2Sm(BH_4)(THF)]$ in the ROP of CL, several other "post-metallocene" early lanthanide borohydride complexes have been reported.[10e,15,16] These include derivatives based on the dianionic, tetradentate ligand N_2NN^* as shown in Figure 7. Analysis of the PCLs (^{1}H NMR and MALDI-TOF) formed with the "post-metallocene" systems confirmed the exclusive formation of α,ω-dihydroxytelechelic chains, OH-PCL. To determine the generality of the results found above for $[Cp_2Eu(BH_4)]$, and to gain insight into the potential effects of using these alternative supporting ligands, we include here a description of the mechanism for the "post-metallocene" system of the type shown in Figure 7.

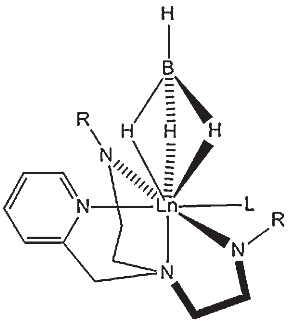

Figure 7. "Post-metallocene" borohydride complexes based on tetradentate diamino-bis(amide) ligands. L = Lewis base or none (dimer); R = $SiMe_3$ or aryl.[15b]

The base-free real systems $[(N_2NN^*)Ln(BH_4)]$ were modeled by using the complex $[(N_2NN')Eu(BH_4)]$ in which the N-substituted N_2NN^* ligand was replaced by the computationally more accessible N-methyl homologue N_2NN' (2-$C_5H_4N)CH_2(CH_2CH_2NMe)_2$. The modeling of N_2NN^* by N_2NN' was validated by comparing the main geometrical features obtained with both borohydride derivatives, namely $[(N_2NN^*)Eu(BH_4)]$ and $[(N_2NN')Eu(BH_4)]$ (**16**, see Table S1 of the Supporting Information). All geometrical parameters and even the charges of the Eu and BH_4^- are beautifully reproduced by the model ligand. As for the metallocene system, the borohydride is η^3 bonded to the lanthanide center, yet with Eu–H distances (2.43, 2.46, and 2.51 Å) longer than for the metallocene system (2.33, 2.45, and 2.46 Å). This is attributed to a stronger negative charge of the N_2NN' ligand with respect to that of the Cp_2 fragment, leading to a smaller negative charge carried by the borohydride ligand. Indeed, an NBO analysis revealed that for both complexes the charge at the metal center is almost identical (+2.5), whereas the charge of the BH_4^- ligands is different (−0.78 for the N_2NN' and −0.90 for the Cp_2), leading to a smaller electrostatic interaction. Thus, the borohydride ligand is less-strongly bonded to the metal fragment with the N_2NN' ligand than with the Cp_2, as confirmed by the calculated heterolytic bond-dissociation energy (139.0 kcal mol^{-1} for $[Cp_2Eu(BH_4)]$ and 122.6 kcal mol^{-1} for $[(N_2NN')Eu(BH_4)]$). This could certainly be generalized to all anionic supporting ligands. Thus, the reactivity of CL with the N_2NN' complex **16**, and more precisely the ring-opening step, could be expected to be less exergonic than the one corresponding to the Cp_2 system, even though breaking the Eu–BH_4 interaction is apparently more facile.

The calculated energy profile for the N_2NN' system is shown in Figure 8 and is very similar to the one obtained for the Cp_2 system (Figure 5). Thus, rather than describing the geometries of all species **16** to **21** (presented in Figure 9) that are very close to those described in Figure 6, we focus on comparing the energetic parameters of the two systems $[Cp_2Eu(BH_4)]$ and $[(N_2NN')Eu(BH_4)]$.

First of all, the reaction is calculated to be kinetically and thermodynamically accessible. The reaction proceeds in two steps as described above for $[Cp_2Eu(X)]$ (X = H or BH_4), and both steps are less exergonic than in the borohydride–metallocene system. This is related to the strong negative charge of the N_2NN' ligand that reduces the charge of the other ligand (see above) and thus that of the electrostatic interaction with the lanthanide center. The effect is rather im-

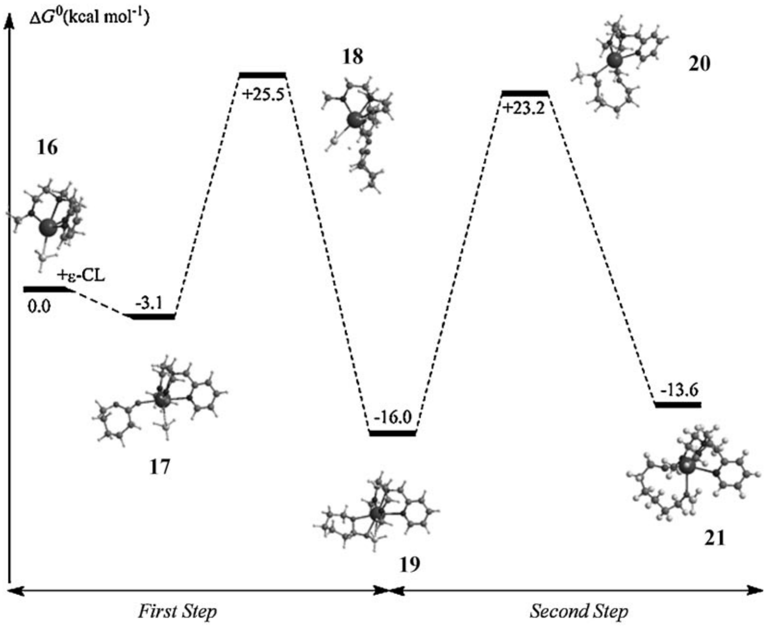

Figure 8. Calculated free-energy profile for the reaction of ε-caprolactone with [$(N_2NN')Eu(BH_4)$].

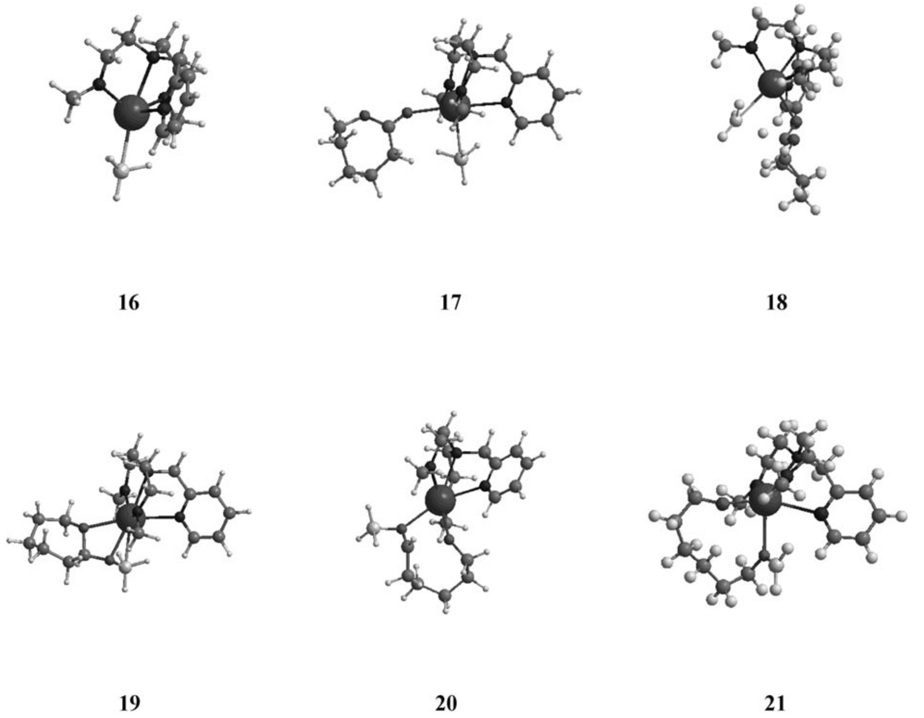

Figure 9. Optimized structures of complexes **16**–**21** involved in the first and second steps of the reaction of CL with [$(N_2NN')Eu(BH_4)$].

portant for the alkoxide complex **21**. Thus, the formation (after ring-opening) of the alkoxide complex **15** in the metallocene system is exergonic by approximately 10 kcal mol^{-1}, whereas in the N_2NN' system it is in thermodynamic equilibrium with complex **19**. Indeed, the charge of the coordinated oxygen atom in the alkoxide complexes is reduced in the N_2NN' system with respect to the metallocene system (−0.84 e and −0.97 e, respectively, at the NBO level), leading to a lower electrostatic interaction with the metal center and thus to a thermodynamically less-favored complex formation. This equilibrium in the last step is similar to that found for the [$Cp_2Eu(H)$] initiator, but the reason is somewhat different.

Thus, as for the hydride catalyst, the polymerization reaction should occur with the N_2NN' ligand. It may seem that N_2NN' might not be the most appropriate ligand to be used for CL polymerization, yet N_2NN' allows a reduction in the electrostatic interaction between the reactive BH_4^- ligand and the metal center. Thus, such a ligand may facilitate the polymerization of MMA (which is experimentally the case),[15b] whereas with the Cp_2 system the cleavage of the lanthanide–borohydride interaction is critical.[14] A theoretical investigation of MMA polymerization using [$(N_2NN')Eu(BH_4)$] is currently underway.

Finally, we note again the excellent agreement between the mechanisms predicted above for both the [$Cp_2Eu(BH_4)$] and [$(N_2NN')Eu(BH_4)$] precursors and the experimental systems that unambiguously showed the formation of di-hydroxy telechelic PCLs. Therefore, one of the terminal CH_2OH groups arises from the presence of an $-CH_2OBH_2$ group on the active polymer chain, which is maintained up to the deactivation/hydrolysis step. The other hydroxyl end group of the macromolecule arises from the deactivation of the Eu−O bond, as depicted in Scheme 2.

Conclusion

In this DFT study we have explored the polymerization-initiation mechanism of ε-caprolactone either by the hydride

$[Cp_2Eu(H)]$ or the borohydrides $[Cp_2Eu(BH_4)]$ and $[(N_2NN')Eu(BH_4)]$. The computational results are fully consistent with experimental studies and, in particular, highlight a number of important differences between *hydride* and *borohydride* as well as between *metallocene and non-metallocene* borohydride precursors. These will aid further research in this topical and important area.

For all of the systems, the reactions proceed with an O−acyl bond cleavage and are predicted to be kinetically and thermodynamically favorable with respect to the separated initiator and CL. We have shown that all three reactions proceed in a stepwise manner via a cyclic alkoxide (or alkoxide–borate) intermediate, and that the ring-opening only occurs in the penultimate step of the initiation process. The $[Cp_2Eu(H)]$ initiator proceeds with inherently lower activation barriers for both the initial hydride-transfer step and the ring-opening second step. This is associated with the greater reorganization required in the BH_4 complexes leading to kinetically slower processes for these latter systems.

The relative stabilities of the cyclic alkoxide intermediates with regard to the ring-opened products was shown to depend on both the initiating group (hydride vs. borohydride) and supporting ligand set (Cp_2 vs. N_2NN'), and leads to a possible equilibrium between cyclic and ring-opened isomers. Therefore, in certain cases ($[Cp_2Eu(H)]$ and $[(N_2NN')Eu(BH_4)]$), the polymerization process should be controlled by the displacement of this final equilibrium and thus, by the experimental conditions. This is not the case for $[Cp_2Eu(BH_4)]$, because the ring-opening step is exergonic. Indeed for both $[Cp_2Eu(BH_4)]$ and $[(N_2NN')Eu(BH_4)]$ this step is fundamentally different to that for the hydride species, as it corresponds to a second B–H activation/hydride migration leading eventually to the formation of a terminal $-CH_2OBH_2$ moiety. In the real polymerization systems this functional group would ultimately be hydrolyzed into a hydroxymethylene terminal group, as observed experimentally.

The alkoxide–borate/ring-opening equilibrium found with the $[(N_2NN')Eu(BH_4)]$ complex arises because of the greater negative charge carried by the N_2NN' ligand relative to Cp_2. This reduces the interaction between the reactive ligands (borohydride or alkoxide) and the metal center. Therefore, use of N_2NN'-type (or other post-metallocene) ligands in conjunction with borohydride initiating groups could allow for the polymerization of a monomer such as MMA in which the key step is to break the interaction between the borohydride and the metal center. Further studies of this and other borohydride-initiated polymerizations are presently underway.

Acknowledgements

N.B. and L.M. would like to thank the CINES and CALMIP for a generous grant of computing time. L.M. is also member of the Institut Universitaire de France. P.M. thanks the EPSRC and Leverhulme Trust for support of the experimental aspects of this research.

[1] a) K. Pang, R. Kotek, A. Tonelli, *Prog. Polym. Sci.* **2006**, *31*, 1009–1037; b) S. Penczek, M. Cypryk, A. Duda, P. Kubisa, S. Slomkowski, *Prog. Polym. Sci.* **2007**, *32*, 247–282; c) A.-C. Albertsson, I. K. Varma, *Biomacromolecules* **2003**, *4*, 1466–1486; d) H. Yasuda, *Prog. Polym. Sci.* **2000**, *25*, 573–626; e) W. Kuran, *Prog. Polym. Sci.* **1998**, *23*, 919–992; f) O. Dechy-Cabaret, B. Matin-Vaca, D. Bourissou, *Chem. Rev.* **2004**, *104*, 6147–6176; g) M. Okada, *Prog. Polym. Sci.* **2002**, *27*, 87–133.

[2] a) M. Vert, *Biomacromolecules* **2005**, *6*, 538–546; b) K. Sudesh, H. Abe, Y. Doi, *Prog. Polym. Sci.* **2000**, *25*, 1503–1555; c) L. S. Nair, C. T. Laurence, *Prog. Polym. Sci.* **2007**, *32*, 762–798.

[3] a) N. E. Kamber, W. Jeong, R. Waymouth, R. C. Pratt, B. G. G. Lohmeijer, J. L. Hedrick, *Chem. Rev.* **2007**, *107*, 5813–5840; b) D. Bourissou, S. Moebs-Sanchez, B. Martin-Vaca, *C. R. Chim.* **2007**, *10*, 775–794; c) O. Coulembier, P. Degée, J. L. Hedrick, P. Dubois, *Prog. Polym. Sci.* **2007**, *31*, 723–747.

[4] a) J. Okuda, *Dalton Trans.*, **2003**, 2367–2378; b) S. Agarwal, C. Mast, K. Dehnicke, A. Greiner, *Macromol. Rapid Commun.* **2000**, *21*, 195–212; c) Z. Hou, Y. Wakatsuki, *Coord. Chem. Rev.* **2002**, *231*, 1–22.

[5] a) Y. Yamashita, E. Takemoto, E. Ihara, H. Yasuda, *Macromolecules* **1996**, *29*, 1798–1806; b) H. Yasuda, E. Ihara, *Bull. Chem. Soc. Jpn.* **1997**, *70*, 1745–1767.

[6] a) V. D. Makhaev, *Russ. Chem. Rev.* **2000**, *69*, 727–746; b) M. Ephritikhine, *Chem. Rev.* **1997**, *97*, 2193–2242; c) T. J. Marks, J. R. Kolb, *Chem. Rev.* **1977**, *77*, 263–293.

[7] Z. Xu, Z. Lin, *Coord. Chem. Rev.* **1996**, *156*, 139–162.

[8] Recent and leading examples: a) A. Y. Khalimon, J. P. Holland, R. M. Kowalczyk, E. J. L. McInnes, J. C. Green, P. Mountford, G. I. Nikonov, *Inorg. Chem.* **2008**, *47*, 999–1006; b) M. Bremer, Nöth, H. M. Warchhold, *Eur. J. Inorg. Chem.* **2003**, 111–119; c) A. Ariafard, M. M. Amini, *J. Organomet. Chem.* **2005**, *690*, 84–95; d) A. Haaland, D. J. Shorokhov, A. V. Tutukin, H. V. Volden, O. Swang, G. S. McGrady, N. Kaltsoyannis, A. J. Downs, C. Y. Tang, J. F. C. Turner, *Inorg. Chem.* **2002**, *41*, 6646–6655; e) N. J. Ashworth, S. L. J. Conway, J. C. Green, M. L. H Green, *J. Organomet. Chem.* **2000**, *609*, 83–88.

[9] a) S. M. Cendrowski-Guillaume, M. Nierlich, M. Lance, M. Ephritikhine, *Organometallics* **1998**, *17*, 786–788; b) S. M. Cendrowski-Guillaume, G. Le Gland, M. Nierlich, M. Ephritikhine, *Organometallics* **2000**, *19*, 5654–5660; c) S. M. Cendrowski-Guillaume, G. Le Gland, M. Lance, M. Nierlich, M. Ephritikhine, *C. R. Chimie* **2002**, *5*, 73–80; d) S. M. Cendrowski-Guillaume, G. Le Gland, M. Ephritikhine, M. Nierlich, *Z. Kristallogr. New Crystal Structures* **2002**, *217*, 35–37.

[10] a) S. M. Guillaume, M. Schappacher, A. Soum, *Macromolecules* **2003**, *36*, 54–60; b) I. Palard, A. Soum, S. M. Guillaume, *Chem. Eur. J.* **2004**, *10*, 4054–4062; c) I. Palard, A. Soum, S. M. Guillaume, *Macromolecules* **2005**, *38*, 6888–6894; d) I. Palard, M. Schappacher, A. Soum, S. M. Guillaume, *Polym. Int.* **2006**, *55*, 1132–1137; e) S. M. Guillaume, M. Schappacher, N. M. Scott, R. Kempe, *J. Polym. Sci. Part A* **2007**, *45*, 3611–3619.

[11] I. Palard, B. Belloncle, M. Schappacher, A. Soum, S. M. Guillaume, *Chem. Eur. J.* **2007**, *13*, 1511–1521.

[12] a) M. Schappacher, A. Soum, S. M. Guillaume, *Biomacromolecules* **2006**, *7*, 1373–1379; b) M. Le Hellaye, N. Fortin, J. Guilloteau, A. Soum, S. Lecommandoux, S. M. Guillaume, *Biomacromolecules* **2008**, in press.

[13] M. Schappacher, N. Fur, S. M. Guillaume, *Macromolecules* **2007**, *40*, 8887–8896.

[14] N. Barros, M. Schappacher, P. Dessuge, L. Maron, S. M. Guillaume, *Chem. Eur. J.* **2007**, *13*, 1881–1890.

[15] a) F. Bonnet, A. R. Cowley, P. Mountford, *Inorg. Chem.* **2005**, *44*, 9046–9055; b) F. Bonnet, A. C. Hillier, A. Collins, S. R. Dubberley, P. Mountford, *Dalton Trans.* **2005**, *44*, 421–423.

[16] a) Y. Nakayama, S. Okuda, H. Yasuda, T. Shiono, *React. Funct. Polym.* **2007**, *67*, 798–806.

[17] a) J. C. Green, *Chem. Soc. Rev.* **1998**, *27*, 263–271; b) P. A. Hunt, *Dalton Trans.* **2007**, 1743–1754; c) L. Perrin, L. Maron, O. Eisenstein, *Inorg. Chem.* **2002**, *41*, 4355–4362; d) L. Maron, L. Perrin, O. Eisenstein, *J. Chem. Soc. Dalton Trans.* **2002**, 534–539; e) E. L. Werkema, E. Messines, L. Perrin, L. Maron, O. Eisenstein, R. A. Andersen, *J. Am. Chem. Soc.* **2005**, *127*, 7781–7795.

[18] a) S. Wang, X. Tang, A. Vega, J.-Y. Saillard, S. Zhou, G. Yang, W. Yao, Y. Wei, *Organometallics*, **2007**, *26*, 1512–1522; b) Y. Luo, P. Selvam, A. Endou, M. Kubo, A. Miyamato, *J. Am. Chem. Soc.* **2003**, *125*, 16210–16212; c) S. Tomasi, H. Weiss, T. Ziegler, *Organometallics* **2006**, *25*, 3619–3630; d) S. Tomasi, H. Weiss, T. Ziegler, *Organometallics* **2007**, *26*, 2157–2166; e) B. Ochiai, T. Endo, *J. Polym. Sci. Part A* **2007**, *45*, 2827–2834; f) N. Buis, S. A. French, G. Ruggiero, B. Stengel, A. A. D. Tulloch, I. H. Williams, *J. Chem. Theory Comput.* **2007**, *3*, 146–155.

[19] M. J. Frisch, G. W. Trucks, H. B. Schlegel, G. E. Scuseria, M. A. Robb, J. R. Cheeseman, J. A. Montgomery, Jr., T. Vreven, K. N. Kudin, J. C. Burant, J. M. Millam, S. S. Iyengar, J. Tomasi, V. Barone, B. Mennucci, M. Cossi, G. Scalmani, N. Rega, G. A. Petersson, H. Nakatsuji, M. Hada, M. Ehara, K. Toyota, R. Fukuda, J. Hasegawa, M. Ishida, T. Nakajima, Y. Honda, O. Kitao, H. Nakai, M. Klene, X. Li, J. E. Knox, H. P. Hratchian, J. B. Cross, V. Bakken, C. Adamo, J. Jaramillo, R. Gomperts, R. E. Stratmann, O. Yazyev, A. J. Austin, R. Cammi, C. Pomelli, J. W. Ochterski, P. Y. Ayala, K. Morokuma, G. A. Voth, P. Salvador, J. J. Dannenberg, V. G. Zakrzewski, S. Dapprich, A. D. Daniels, M. C. Strain, O. Farkas, D. K. Malick, A. D. Rabuck, K. Raghavachari, J. B. Foresman, J. V. Ortiz, Q. Cui, A. G. Baboul, S. Clifford, J. Cioslowski, B. B. Stefanov, G. Liu, A. Liashenko, P. Piskorz, I. Komaromi, R. L. Martin, D. J. Fox, T. Keith, M. A. Al-Laham, C. Y. Peng, A. Nanayakkara, M. Challacombe, P. M. W. Gill, B. Johnson, W. Chen, M. W. Wong, C. Gonzalez, J. A. Pople, Gaussian 03, Revision B.05, Gaussian, Inc., Wallingford CT, **2004**.

[20] a) M. Dolg, H. Stoll, A. Savin, H. Preuss, *Theor. Chim. Acta* **1989**, *75*, 173–194; b) M. Dolg, H. Stoll, H. Preuss, *Theor. Chim. Acta* **1993**, *85*, 441–450.

[21] L. Maron, O. Eisenstein, *Phys. Chem. A* **2000**, *104*, 7140–7143.

[22] W. J. Hehre, R. Ditchfield, J. A. Pople, *J. Chem. Phys.* **1972**, *56*, 2257–2261.

[23] a) J. P. Perdew, Y. Wang, *Phys. Rev. B* **1992**, *45*, 284; b) A. D. Becke, *J. Chem. Phys.* **1993**, *98*, 5648–5652.

[24] a) A. Hofman, S. Slomkowski, S. Penczek, *Makromol. Chem.* **1984**, *185*, 91–101; b) H. B. Burgi, J. D. Dunitz, J. M. Lehn, G. Wipff, *Tetrahedron* **1974**, *30*, 1563–1572.

[25] L. Perrin, L. Maron, O. Eisenstein, *New J. Chem.* **2004**, *28*, 1255–1259.

[26] E. L. Werkema, L. Maron, O. Eisenstein, R. A. Andersen, *J. Am. Chem. Soc.* **2007**, *129*, 2529–2541.

[27] a) M. T. Gamer, P. W. Roesky, I. Palard, M. Le Hellaye, S. M. Guillaume, *Organometallics* **2007**, *26*, 651–657; b) H. Ma, T. P. Spaniol, J. Okuda, *Dalton Trans.* **2003**, 4770–4780; c) Y. Shen, Z. Shen, Y. Zhang, K. Yao, *Macromolecules* **1996**, *29*, 8289–8295; d) F. M. Kerton, A. C. Withwood, C. E. Williams, *Dalton Trans.* **2004**, 2237–2244.

[28] This TS is hard to locate and was obtained by scanning the potential-energy surface (PES) between the adduct and the product.

Received: March 3, 2008